A high-pressure structural study of potassium titanyl phosphate (KTP) up to 5 GPa

1992 J. Phys.: Condens. Matter 4 2747

(http://iopscience.iop.org/0953-8984/4/11/005)

J. Phys.: Condens. Matter 4 (1992) 2747–2760. Printed in the UK

A high-pressure structural study of potassium titanyl phosphate (KTP) up to 5 GPa

D R Allan†, J S Loveday†, R J Nelmes† and P A Thomas‡

† Department of Physics, The University of Edinburgh, Mayfield Road, Edinburgh EH9 3JZ, UK

‡ Department of Physics, University of Warwick, Coventry CV4 7AL, UK

Received 4 July 1991, in final form 29 October 1991

Abstract. The crystal structure of $KTiOPO_4$ (KTP) has been determined as a function of pressure up to 5 GPa at room temperature, using x-ray diffraction techniques and a single-crystal sample. The principal changes with pressure are in the coordination environments of the potassium atoms and in the linking angles of the TiO_6–PO_4 structural framework. In general the distortions of the TiO_6 octahedra, which have been linked to the second harmonic generating properties of KTP, are retained although there are some small changes in the Ti–O bond lengths. The overall structural changes are consistent with a first-order character for the phase transition at 5.5 GPa.

1. Introduction

Potassium titanyl phosphate, $KTiOPO_4$ (KTP), exhibits highly non-linear optical properties and is finding an increasing number of applications in the field of optoelectronics. At room temperature the structure of KTP assumes the acentric $Pna2_1$ space group with lattice parameters $a = 12.819(3)$ Å, $b = 6.399(1)$ Å, $c = 10.584(2)$ Å, $V = 868.1$ Å^3 [1]. The principal structural origin of this non-linear optical behaviour has been considered to be the anomalously short Ti–O bonds in the highly distorted TiO_6 octahedra [2], which form characteristic chains in the [011] and [0$\bar{1}$1] directions, linked by alternately long and short Ti–O bonds (e.g. the chain A, B, C, D, E in figure 1). Several structural analogues of KTP have been reported where K is substituted by (for example) Rb or Tl [3], P by As [4] and more recently where Ti is substituted by (for example) Sn [5] or Fe [6]. All of these have been extensively reviewed [7]. The KTP structure shows a pronounced pseudosymmetry derived from the centric $Pnan$ space group and recently the thallium analogue $TlTiOPO_4$ (TTP) has been reported to undergo a transition into this $Pnan$ symmetry at 923 K [8]. In addition to this, a high-pressure Raman study of KTP, carried out by Kourouklis *et al* [9], provides evidence of a phase transition at 5.5 GPa to an, as yet, uncharacterized phase. This Raman study shows that there is an increase in the number of modes at the 5.5 GPa phase transition, which indicates a lowering of the symmetry or a multiplication of the unit cell. The mechanism of the transition is proposed to be polyhedral tilting in the TiO_6–PO_4 framework being driven by the softening low-frequency Raman mode near 56 cm^{-1}. This mode, which has been associated with the potassium atoms [10], has a small discontinuity at the phase transition, indicating that the transition is weakly

0953-8984/92/112747+14$04.50

first order. On release of pressure the original Raman spectrum appears with no microscopic change in the appearance of the sample. This indicates that although the transition is first order it is reversible. A high-pressure structural study of KTP was mentioned briefly towards the end of a review article by Stucky *et al* [7] although it has not been reported in more detail elsewhere. No structural results are given apart from a bond angle change of 6.1° at 1 GPa for an unspecified P–O–Ti linking bond. In the absence of any other information regarding the pressure dependence of KTP the present investigation was undertaken to establish the major structural changes occurring as the phase transition at 5.5 GPa is approached.

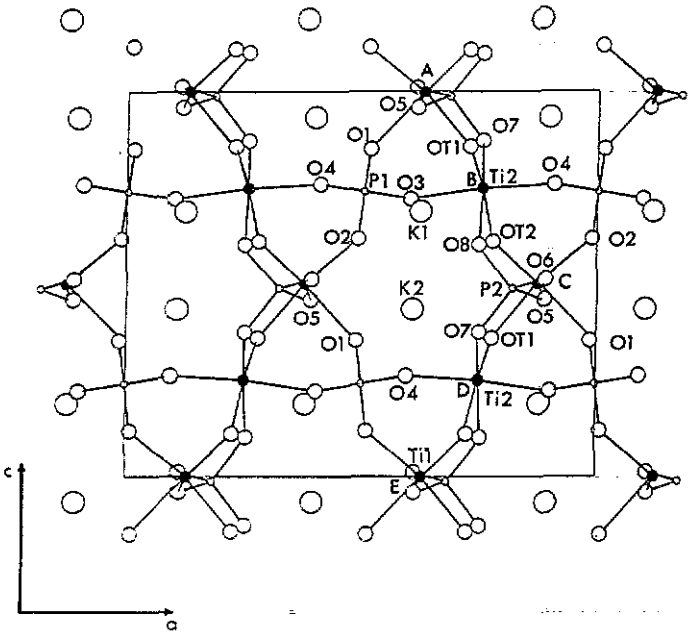

Figure 1. The structure of $KTiOPO_4$ viewed along the *b*-axis. The shaded circles represent the titanium atoms and the atoms labelled A, B, C, D, E are titanium atoms forming a chain linked by alternately long and short Ti–OT bonds.

2. The experiment and data analysis

A single crystal of flux-grown KTP was cut to the approximate dimensions of 100 μm × 100 μm × 100 μm and the resulting fragment was mounted and centred on a CAD4 four-circle diffractometer. The crystal quality was then checked and the crystallographic axes determined relative to the somewhat irregular crystal shape. A series of ψ scans was also performed to ensure that the crystal absorption had been adequately characterized. The data were to be collected using a Merrill–Bassett diamond-anvil pressure cell (DAC) which limits the region of accessible reflections to that lying close to the reciprocal lattice plane parallel to the diamond-anvil faces. In order to determine how the crystal should be mounted in the DAC, a series of trial refinements was performed on a previously collected three-dimensional ambient data set, taking the structural parameters of Thomas *et al* [1] as starting values. Regions of

inaccessible reflections were removed from the data to simulate the crystal mounted with either the a-, b- or c-axes perpendicular to the plane of the diamond-anvil face. The results of these refinements indicated that the lowest correlations between the positional parameters were observed for the a-axis setting. It was also found that the errors for the x-coordinates were not significantly higher than those for the y- and z-coordinates despite the a-axis being the direction of lowest resolution in the restricted data set. Therefore, it was decided to mount the crystal with its a-axis perpendicular to the diamond-anvil face.

The sample was secured to one diamond face, using petroleum jelly, with chips of ruby placed beside it for pressure calibration. The DAC was then assembled with a tungsten gasket confining the sample and a 4:1 methanol–ethanol fluid (dried with molecular sieve) used to transmit the pressure. Initially the cell was taken to a very low pressure of 0.2 GPa (measured to ± 0.05 GPa using the ruby fluorescence method) which is just adequate to ensure the cell is firmly sealed and the crystal mounting secure. The DAC was centred on the CAD4 and the sample carefully aligned using graphite-monochromated Ag Kα x-rays. This wavelength was chosen due to the superior resolution and lower absorption it offers over Mo Kα [11].

A low-pressure reference data set was then collected, measuring each reflection with the ω-scan method at the position of least attenuation by the pressure cell, according to the procedure of Finger and King [12]. The reflections were also measured at three positions over a narrow range around the scattering vector to detect and eliminate errors due to simultaneous diffraction by the diamond anvils [13]. Initially data were carefully collected in the region of $0° < \theta < 15°$ and, with a slightly increased scan speed, in the region of $15° < \theta < 30°$. At least two equivalents were present $(\pm h, -k, \pm l)$ in both shells. Reflections for which either the incident or reflected beam lay beyond 37° from the cylindrical symmetry axis of the cell were not collected, leaving a small safety margin on the limit (40°) imposed by the steel mounting of the beryllium discs [4]. All reflections affected by simultaneous diamond reflections were removed from the data set. After applying a correction for the absorption of both the pressure cell [12, 14] and the sample, the data were averaged over repeated measurements and used for an initial least-squares refinement of the structure, including an extinction correction, using the Prometheus crystallographic programs [15]. The structural parameters obtained by Thomas *et al* [1] were taken as starting values. It became apparent that since many of the reflections were relatively weak, particularly for the second shell, it was very important that the most structurally sensitive of these weak reflections were identified and their intensities measured more accurately. This was achieved with the 'leverage' procedure [16] as implemented by Hazen and Finger [17], which uses the derivatives calculated by the least-squares program to identify reflections most sensitive to the variable parameters of interest. The intensities of the 'leveraged' reflections were then remeasured with increased counting times, to improve their precision, and added to the data set. Structure factors were calculated for the remaining accessible reflections and for reflections whose intensities had not already been measured accurately. The strong and intermediate reflections predicted from these calculations were measured, as accurately as the 'leveraged' reflections, and added to the data set. All of the poorly determined reflections $(I < 3\sigma(I))$ present in the second shell were removed from the refinement. This had little effect on either the refined coordinates or on the magnitude of their errors. The resulting data set, which covers the whole range of accessible reflections (up to $\sin\theta/\lambda = 1.0$ Å^{-1}), was then used for a final least-squares

structural refinement. As for the initial refinement, all the reflections not rejected due to simultaneous diamond reflections were corrected for pressure-cell and sample absorption and averaged over identical reflections. In order to assign weights correctly to the reflections in the data set, averaging over the equivalent reflections and leveraged reflections only occurred after the final structural refinement. In the least-squares refinement each reflection was assigned a weight $w = 1/[\sigma^2(F_o) + f]$, where $\sigma(F_o)$ is the ESD for the observed structure factor and f is an estimate of the irreducible uncertainties in the measurement of intensities [18] (taken in this case to be 3% of the observed intensity of each reflection). Averaging over the equivalent reflections after the refinement allowed the internal consistency of the data to be determined.

The positional parameters for all of the atoms refined stably with no significant correlations between them. However, due to the rather limited data set, this was not found to be the case for the thermal parameters, and various constraints had to be applied. For all except the potassium atoms, only isotropic temperature factors were refined. This seems appropriate since the ambient structural study, carried out by Thomas *et al* [1], demonstrates that the potassiums are the only atoms exhibiting significantly anisotropic thermal motion: the other atoms, which form the TiO_6–PO_4 framework, have thermal motions which are almost isotropic. A further constraint was introduced by holding the anisotropic thermal parameters directed along a (the direction of lowest resolution in the data) to their ambient values. With all these constraints applied, the refinement converged and gave physically reasonable thermal parameters for the K, Ti and P atoms. However, the oxygen atoms were less well defined and additional constraints had to be applied to them. Since the oxygen atoms all have similar environments, their isotropic thermal parameters were all constrained to be the same, except for those involved in the short Ti–O bonds (labelled OT1 and OT2). The parameters for these two atoms were kept the same as each other, but allowed to differ from the other oxygens. In order to determine the effect of these further constraints, Hamilton's R-factor test [19] was applied between refinements where the oxygen thermal parameters were allowed to refine freely and where they were constrained. The test revealed that the constraints changed the R-factor by less than the 90% confidence limit and are therefore not statistically significant for the data [20]. The refined positional parameters were also found to agree to within 1.5σ or better, indicating that the constraints had not biased the refinement significantly. Physically reasonable values were then obtained for all the thermal parameters although the errors were fairly large. The anisotropic thermal parameters for the potassium atoms agreed with the values obtained by Thomas *et al* [1] to within 20% while the isotropic thermal parameters for the other atoms agreed with Trodjman *et al* [2] to within a factor of two. As a final check that the thermal-parameter constraints did not affect the positional parameters, a full data set, measured at ambient pressure, was refined with anisotropic thermal parameters for all the atoms. The results were compared with a second refinement where the above constraints had all been applied, and there were no significant differences between the positional parameters for the two refinements (all agreeing to within σ).

The purpose of the low-pressure reference data set was to determine to what extent (if at all) the restrictions imposed by the pressure cell bias the data, as well as establishing a reasonable data-collection strategy. Any bias in the data may result in some small offsets in the refined positional parameters from their ambient pressure values. The low-pressure reference data set therefore provides a secure starting point

from which any changes in the structure can be determined from data measured at higher pressures.

Data were collected for pressures of 2.2, 3.7 and 4.7 GPa following the strategy already outlined for the 0.2 GPa reference data and at each pressure, including 0.2 Gpa, (i) the unit-cell dimensions were determined accurately by the four-equivalent-settings procedure of King and Finger [21] which corrects for any sample miscentring, and (ii) the pressure was remeasured after the data collection to ensure it had remained constant. Again the data were corrected for pressure-cell and crystal absorption and averaged over identical reflections. As already explained, averaging over equivalent reflections was carried out after the final refinements and allowed the internal consistency of each data set to be determined.

3. Results and discussion

Table 1 presents the refined atomic coordinates, the measured unit-cell dimensions and unit-cell volume, the number of independent reflections, the number of refined parameters and the goodness-of-fit expressed as an R-factor. The results of the atmospheric-pressure study conducted by Thomas *et al* [1] are also given for comparison. All the R-factors for the high-pressure data are similar and the refined scale factors (not given) show only a small monotonic variation in the sequence in which the data were collected. The bond lengths of the K cages, Ti octahedra and P tetrahedra derived from these refinements are given in table 2.

The unit-cell volume is plotted as a function of pressure in figure 2. A Murnaghan fit to the values, using the Volfit program [22], yields a bulk modulus $B_0 = 58 \pm 8$ GPa with a curvature of $B' = 15 \pm 4$. The unit-cell volume decreases by 2.8(1)% at 2.2 GPa, comparable with that of the anorthite feldspar ($CaAl_2Si_2O_8$) which exhibits a decrease of 2.8(1)% at 2.5 GPa [23]. Anorthite has similar structural properties to those of KTP and will be described in more detail later.

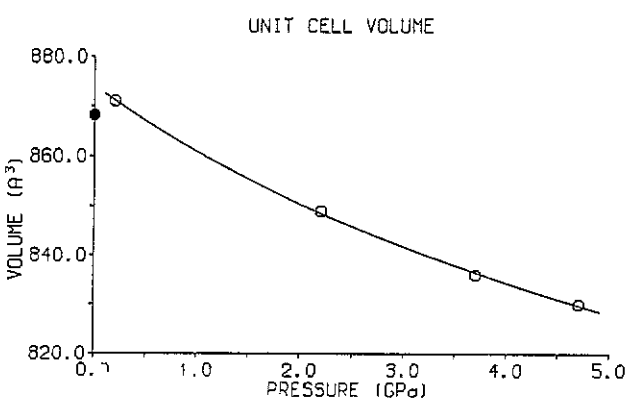

Figure 2. The unit-cell volume of $KTiOPO_4$ as a function of pressure. The atmospheric-pressure value, shown as ●, is calculated from the unit-cell dimensions of Thomas *et al* [1]. Note that errors are smaller than the symbols shown. The line is fitted to the high-pressure points using a Murnaghan function.

Table 1. Unit-cell dimensions (Å), unit-cell volume (Å^3) and refined atomic fractional coordinates of $KTiOPO_4$ as a function of pressure. The number of independent reflections (N_i), the number of refined parameters (N_r) and the weighted R factor (R_w) are also given. The R-factor for the refinements is defined as follows:

$$R_w = \left(\frac{\sum_N w(F_o - F_c)^2}{\sum_N w F_o^2} \right)^{1/2}$$

where N is the number of refined reflections and w is the weight assigned to each reflection. The estimated standard deviations (ESDs) for each of the values are given in parentheses. Note that the Prometheus refinement program requires that one atom be fixed along the polar axis. The Ti1 z coordinate was chosen to be fixed, and so no ESD is quoted for it. The atmospheric-pressure (AP) values were calculated from the refined atomic fractional coordinates of Thomas *et al* [1].

		Pressure (GPa)				
		AP [1]	0.2 GPa	2.2 GPa	3.7 GPa	4.7 GPa
	a (Å)	12.819(3)	12.832(7)	12.705(7)	12.639(7)	12.620(8)
	b (Å)	6.399(1)	6.412(3)	6.363(2)	6.331(2)	6.315(4)
	c (Å)	10.584(2)	10.586(4)	10.505(4)	10.447(4)	10.417(5)
	V (Å^3)	868.1(4)	871(1)	849(1)	836(1)	830(1)
K1	x	0.378 07(8)	0.3795(5)	0.3813(5)	0.3815(5)	0.3818(4)
	y	0.7806(1)	0.7799(5)	0.7796(5)	0.7807(5)	0.7819(5)
	z	0.6880(1)	0.6867(4)	0.6860(4)	0.6855(4)	0.6853(5)
K2	x	0.105 26(7)	0.1049(6)	0.1049(6)	0.1045(5)	0.1046(4)
	y	0.6990(1)	0.6989(5)	0.6946(5)	0.6921(4)	0.6911(5)
	z	0.9332(1)	0.9331(6)	0.9325(5)	0.9332(5)	0.9320(6)
Ti1	x	0.372 90(4)	0.3737(4)	0.3728(3)	0.3733(3)	0.3743(3)
	y	0.5001(1)	0.5013(5)	0.5004(4)	0.5013(4)	0.5006(4)
	z	−0.00040(8)	−0.0004	−0.0004	−0.0004	−0.0004
Ti2	x	0.246 58(6)	0.2450(6)	0.2450(5)	0.2467(5)	0.2461(4)
	y	0.2695(5)	0.2697(4)	0.2690(4)	0.2686(3)	0.2685(3)
	z	0.748 36(9)	0.7483(5)	0.7480(5)	0.7484(5)	0.7486(6)
P1	x	0.498 08(8)	0.4986(8)	0.4981(8)	0.4980(7)	0.4970(6)
	y	0.3363(1)	0.3360(4)	0.3338(4)	0.3318(4)	0.3318(4)
	z	0.7397(1)	0.7409(6)	0.7419(6)	0.7409(5)	0.7404(6)
P2	x	0.180 79(7)	0.1822(6)	0.1815(6)	0.1805(5)	0.1797(5)
	y	0.5020(1)	0.5000(9)	0.5003(7)	0.5029(8)	0.5024(6)
	z	0.4872(1)	0.4882(6)	0.4874(5)	0.4882(5)	0.4891(6)
O1	x	0.4859(2)	0.4852(14)	0.4873(12)	0.4868(13)	0.4890(12)
	y	0.4867(5)	0.4894(12)	0.4863(12)	0.4873(12)	0.4857(13)
	z	0.8497(2)	0.8478(9)	0.8522(8)	0.8500(9)	0.8481(11)
O2	x	0.5103(2)	0.5142(17)	0.5087(13)	0.5094(14)	0.5100(10)
	y	0.4657(5)	0.4616(12)	0.4604(12)	0.4583(13)	0.4600(13)
	z	0.6170(2)	0.6168(8)	0.6146(8)	0.6162(8)	0.6174(11)

Table 1. (Continued)

		Pressure (GPa)				
		AP [1]	0.2 GPa	2.2 GPa	3.7 GPa	4.7 GPa
O3	x	0.4004(2)	0.4009(12)	0.4023(12)	0.4009(12)	0.4004(9)
	y	0.1986(4)	0.2037(13)	0.1981(14)	0.1920(14)	0.1897(13)
	z	0.7208(2)	0.7192(10)	0.7234(9)	0.7226(10)	0.7272(13)
O4	x	0.5934(2)	0.5908(15)	0.5929(14)	0.5918(14)	0.5917(11)
	y	0.1930(4)	0.1888(13)	0.1851(13)	0.1836(13)	0.1840(14)
	z	0.7589(2)	0.7572(9)	0.7590(9)	0.7583(10)	0.7574(11)
OT1	x	0.2248(2)	0.2226(14)	0.2233(14)	0.2273(13)	0.2274(12)
	y	0.9653(4)	0.9694(16)	0.9714(15)	0.9737(14)	0.9703(15)
	z	0.3561(2)	0.3537(10)	0.3537(9)	0.3354(9)	0.3566(11)
OT2	x	0.2232(2)	0.2195(17)	0.2205(14)	0.2218(14)	0.2219(12)
	y	0.0413(5)	0.0423(18)	0.0388(17)	0.0428(15)	0.0407(15)
	z	0.6097(2)	0.6088(12)	0.6097(11)	0.6119(10)	0.6126(11)
O5	x	0.1126(2)	0.1118(14)	0.1089(14)	0.1126(11)	0.1094(10)
	y	0.3106(4)	0.3162(13)	0.3141(12)	0.3177(12)	0.3143(12)
	z	0.4585(2)	0.4560(10)	0.4545(9)	0.4574(10)	0.4594(15)
O6	x	0.1113(2)	0.1119(15)	0.1120(15)	0.1087(15)	0.1083(13)
	y	0.6918(4)	0.6938(13)	0.6904(12)	0.6961(12)	0.6937(13)
	z	0.5117(3)	0.5129(11)	0.5127(9)	0.5124(10)	0.5126(12)
O7	x	0.2525(2)	0.2506(17)	0.2551(17)	0.2575(15)	0.2560(13)
	y	0.5402(5)	0.5420(16)	0.5415(15)	0.5364(15)	0.5419(15)
	z	0.3718(2)	0.3713(10)	0.3720(9)	0.3734(10)	0.3747(11)
O8	x	0.2528(2)	0.2522(14)	0.2560(11)	0.2542(12)	0.2536(12)
	y	0.4619(5)	0.4598(16)	0.4598(14)	0.4602(15)	0.4602(16)
	z	0.6008(2)	0.6014(12)	0.6003(10)	0.6015(11)	0.6006(12)
	N_i	2158	490	491	496	417
	N_r	145	65	65	65	65
	R_w	0.024	0.044	0.042	0.047	0.051

From table 1 it is clear that the K2 atom exhibits a shift under pressure while the K1 atom remains relatively stationary. To illustrate this, their fractional coordinates are plotted as a function of pressure in figure 3. The potassium atoms occupy cavities, or cages, in the TiO_6–PO_4 framework and are loosely held in the structure. The movement of the K2 atom suggests that its cage exhibits a significant pressure dependence. This pressure dependence will manifest itself as a relative movement in the TiO_6–PO_4 framework and, upon examination of table 1, it is evident that the P1, P2 and O3 atoms undergo clear shifts. To illustrate the shifts, the fractional coordinate changes for the P1 and O3 atoms are also shown in figure 3 (note that P2 has a shift of similar magnitude to that of P1 and is not shown in the figure). The small but significant offset of the O3 y-coordinate at 0.2 GPa from the atmospheric-pressure value illustrates the need for the low-pressure reference data set in determining trends in the structure.

Table 2. The bond lengths (Å) of the K cages, Ti octahedra and P tetrahedra in $KTiOPO_4$ as a function of pressure. The atmospheric-pressure (AP) values were calculated from the refined atomic fractional coordinates of Thomas *et al* [1].

		Pressure (GPa)				
		AP [1]	0.2 GPa	2.2 GPa	3.7 GPa	4.7 GPa
$K(1)O_8$	K1–O1	2.894(4)	2.867(12)	2.889(11)	2.859(11)	2.865(12)
	K1–O2	2.738(4)	2.775(16)	2.703(13)	2.702(14)	2.693(12)
	K1–O3	2.712(3)	2.753(10)	2.705(10)	2.644(10)	2.622(10)
	K1–O5	2.872(3)	2.862(10)	2.832(9)	2.851(10)	2.864(15)
	K1–O7	3.057(3)	3.071(14)	3.099(15)	3.092(12)	3.100(13)
	K1–O8	2.755(4)	2.774(15)	2.736(11)	2.734(13)	2.743(13)
	K1–OT1	2.995(3)	2.967(12)	2.953(12)	2.969(11)	2.992(12)
	K1–OT2	2.722(4)	2.780(19)	2.745(16)	2.724(16)	2.705(13)
$K(2)O_9$	K2–O1	2.677(3)	2.677(12)	2.658(12)	2.663(15)	2.656(11)
	K2–O2	2.982(3)	2.991(14)	2.933(11)	2.927(12)	2.950(12)
	K2–O3	3.045(3)	3.029(11)	3.057(10)	3.024(11)	3.075(12)
	K2–O4	3.117(3)	3.112(9)	3.031(8)	3.003(9)	2.991(10)
	K2–O5	2.806(3)	2.793(19)	2.727(18)	2.757(16)	2.717(14)
	K2–O7	2.918(4)	2.951(15)	2.905(14)	2.861(14)	2.891(13)
	K2–O8	3.048(4)	3.055(16)	3.013(14)	3.027(14)	3.028(14)
	K2–OT1	2.765(4)	2.789(15)	2.733(15)	2.663(15)	2.656(15)
	K2–OT2	3.057(4)	3.089(22)	3.062(17)	3.033(17)	3.039(15)
$Ti(1)O_6$	Ti1–O1	2.150(3)	2.153(13)	2.126(12)	2.123(13)	2.144(14)
	Ti1–O2	1.958(3)	1.915(17)	1.946(14)	1.936(15)	1.923(13)
	Ti1–O5	2.042(3)	2.079(8)	2.065(8)	2.058(8)	2.035(9)
	Ti1–O6	1.987(3)	1.985(8)	1.986(8)	1.950(8)	1.956(9)
	Ti1–OT1	1.981(3)	1.988(14)	1.968(13)	1.978(13)	1.975(13)
	Ti1–OT2	1.716(3)	1.684(17)	1.675(13)	1.700(13)	1.710(13)
$Ti(2)O_6$	Ti2–O3	2.044(3)	2.067(15)	2.065(16)	2.026(15)	2.022(11)
	Ti2–O4	1.981(3)	1.999(16)	1.958(17)	1.983(17)	1.974(13)
	Ti2–O7	1.965(3)	1.957(11)	1.948(10)	1.967(10)	1.942(10)
	Ti2–O8	1.990(3)	1.978(11)	1.975(10)	1.958(10)	1.963(11)
	Ti2–OT1	1.733(3)	1.749(12)	1.748(10)	1.745(10)	1.732(11)
	Ti2–OT2	2.092(3)	2.101(12)	2.086(11)	2.043(11)	2.042(11)
$P(1)O_4$	P1–O1	1.519(3)	1.509(10)	1.517(9)	1.513(9)	1.489(12)
	P1–O2	1.548(3)	1.554(9)	1.567(9)	1.537(9)	1.525(12)
	P1–O3	1.544(3)	1.531(15)	1.505(15)	1.525(14)	1.520(12)
	P1–O4	1.541(3)	1.523(17)	1.542(18)	1.523(17)	1.527(13)
$P(2)O_4$	P2–O5	1.535(3)	1.523(15)	1.540(14)	1.488(13)	1.515(10)
	P2–O6	1.528(3)	1.557(14)	1.521(15)	1.544(15)	1.526(12)
	P2–O7	1.548(3)	1.541(15)	1.553(16)	1.559(14)	1.553(14)
	P2–O8	1.537(3)	1.520(13)	1.539(12)	1.530(13)	1.513(13)

In order to determine the relative compressibilities of the K cages, the PO_4 tetrahedra and the TiO_6 octahedra, their volumes were calculated for all four pressures by dividing each unit into constituent irregular tetrahedra. The PO_4 tetrahedra and TiO_6 octahedra require one and four such tetrahedra respectively, with an oxygen atom at each vertex. For the K cage sites the consituent tetrahedra were determined

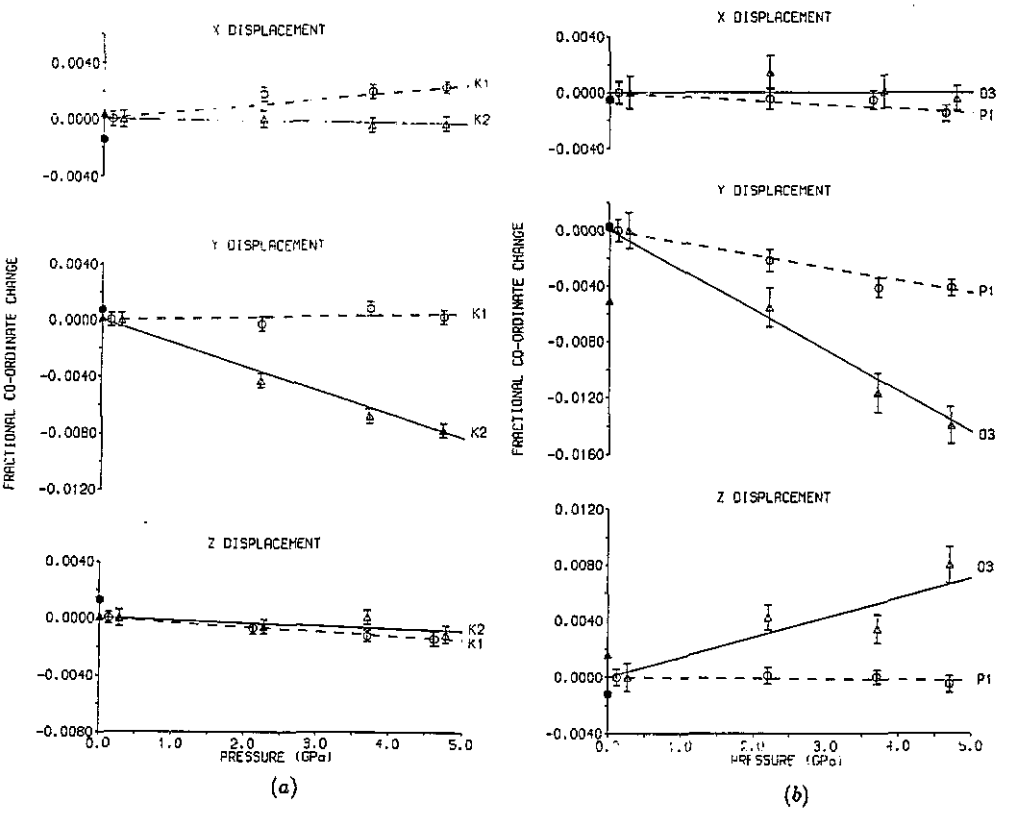

Figure 3. (*a*) Fractional coordinate changes for the K1 (○) and K2 (△) atoms, and (*b*) for the P1 (○) and O3 (△) atoms in $KTiOPO_4$ relative to the 0.2 GPa values. The atmospheric-pressure values, shown as ● and ▲, are from Thomas *et al* [1]. Note that some of the points have been translated slightly along the pressure axis to avoid overlap. The broken and full lines are a guide to the eye only.

by placing a K atom at one vertex and neighbouring oxygen atoms at the remaining three vertices. Describing the volume of the cage sites in this way requires twelve and fourteen such tetrahedra for the $K(1)O_8$ and $K(2)O_9$ cages respectively. The volume of each of the irregular tetrahedra can be readily calculated from the appropriate bond lengths and bond angles and then summed to yield the volume of each structural unit. As can be seen from table 3, all the units show a decrease in volume under pressure, although their relative volume changes are quite different: the K cages have a $5.7 \pm 1\%$ reduction in volume at 4.7 GPa, while the Ti octahedra and P tetrahedra have $2.8 \pm 2\%$ and $2.4 \pm 2\%$ reductions respectively. Therefore, it seems that the large potassium cage sites are readily compressible and absorb a significant fraction of the overall $4.7 \pm 0.2\%$ reduction in the unit-cell volume at 4.7 GPa. The average volume change of the K cage sites is plotted in figure 4 along with the change in the unit-cell volume. It is evident from figure 4 that the curvature of the pressure–volume relationship is significantly greater for the K cages than for the unit cell.

From figure 1, which presents the structure of KTP projected along the *b*-axis, it is evident that the environments for the K1 and K2 atoms are quite different. The $K(2)O_9$ cage forms a channel, parallel to the *b*-axis, which runs through the entire crystal structure and along which the K2 atom may be expected to move relatively

Table 3. The pressure dependence of the average M–O bond lengths (Å) in the TiO_6 octahedra, PO_4 tetrahedra and K cages of $KTiOPO_4$ and of the volumes (Å^3) of these structural units. The definition of the volumes is discussed in the text. The atmospheric-pressure (AP) values were calculated from the refined atomic fractional coordinates of Thomas *et al* [1].

	Pressure (GPa)				
	AP [1]	0.2 GPa	2.2 GPa	3.7 GPa	4.7 GPa
TiO_6 octahedra					
Average bond length (Å)	1.970(3)	1.971(13)	1.962(12)	1.956(12)	1.952(12)
Volume (Å^3)	10.08(5)	10.08(18)	9.94(17)	9.86(17)	9.80(16)
PO_4 tetrahedra					
Average bond length (Å)	1.537(3)	1.532(13)	1.534(13)	1.527(13)	1.521(12)
Volume (Å^3)	1.86(1)	1.84(5)	1.86(5)	1.83(5)	1.80(4)
K1 cage					
Average bond length (Å)	2.843(4)	2.856(14)	2.833(12)	2.822(12)	2.823(12)
Volume (Å^3)	26.15(6)	26.46(36)	25.72(33)	25.14(34)	25.00(31)
K2 cage					
Average bond length (Å)	2.934(3)	2.943(15)	2.902(13)	2.884(14)	2.889(13)
Volume (Å^3)	34.71(7)	35.12(45)	33.46(45)	32.91(45)	33.03(45)

freely; and it is seen in figure 3 that the only significant movement of the K2 atom with increasing pressure is along the *b*-axis (i.e. along the channel). On the other hand, the K1 atom is constrained from a similar motion by the confinement of the $P(1)O_4$–$Ti(2)O_6$ chain which restricts movement of the K1 atom along the *b*-axis (see figure 1). It is interesting to note that although the K1 cage forms a channel which runs parallel to the *a*-axis, the K1 atom does not show a significant movement along the *a*-axis with increasing pressure. The apparent difference in behaviour may be partly due to the greater restriction offered by the K1 cage environment, which has a volume 25% smaller than that of the K2 cage. There is also a significant difference in compressibility in the average K–O bond lengths which reduce by $1.2 \pm 0.3\%$ and $1.8 \pm 0.2\%$ for the K1 and K2 cages respectively.

As the $P(1)O_4$–$Ti(2)O_6$ chain deforms under pressure, the motion of the O3 atom, combined with that of the P1 atom, results in a reduction of the P1–O3–Ti2 bond angle by approximately 3° between 0.2 and 4.7 GPa (see table 4). This bond links the chain of alternate $P(1)O_4$ tetrahedra and $Ti(1)O_6$ octahedra which is directed along the *a*-axis (see figure 1). The most significant TiO_6–PO_4 linking angle change, however, is in the P2–O7–Ti2 bond which reduces by approximately 5° over the same pressure range (see table 4). (This is less than 20% of the angular change of 6.1° at 1 GPa reported by Stucky *et al* [7] for an unspecified P–O–Ti bond.) All the other P–O–Ti bonds have angular changes of approximately 2° or less, as do the Ti–OT–Ti bonds which link the titanium octahedra (the P1–O4–Ti2, P2–O6–Ti1 and Ti1–OT2–Ti2 linking bonds are given as examples in table 4).

The overall distortion of the $Ti(1)O_6$ and $Ti(2)O_6$ octahedra appears to be retained up to 4.7 GPa in as much as the general pattern of long and short Ti–O bond lengths remains the same (as can be seen from table 2) and the O–Ti–O bonds, within the octahedra, have angular changes of only 2° or less. The anomalously short Ti–OT

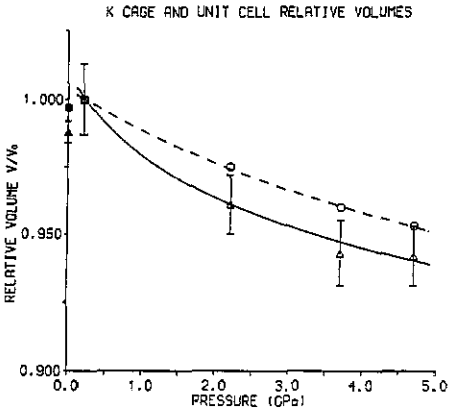

Figure 4. The relative volumes (V/V_0) of the unit-cell volume (○) and K cages (△) (the K1 and K2 cages averaged) in $KTiOPO_4$ as a function of pressure, referred to the value V_0 at 0.2 GPa. The atmospheric-pressure values, shown as ● and ▲, are calculated from the unit-cell dimensions and the fractional coordinates of Thomas *et al* [1]. Note that where error bars are not shown, the errors are smaller than the circular symbols. The broken and full curves are from Murnaghan fits to the relative volumes of the unit cell and the K cages respectively.

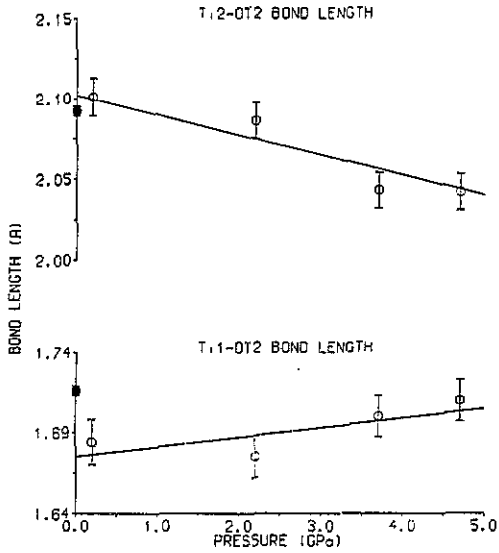

Figure 5. The Ti2–OT2 and Ti1–OT2 bond lengths in $KTiOPO_4$ as a function of pressure. The atmospheric-pressure values, shown as ●, are calculated from the fractional coordinates of Thomas *et al* [1]. The lines indicate the changes in the bonds and are a guide to the eye only.

bonds within the highly distorted TiO_6 octahedra have been considered to be linked to the non-linear optical properties of KTP and are consequently of great interest [2]. From table 2 it is evident that the Ti1–OT2 and Ti2–OT2 bond lengths both undergo systematic changes under pressure. The longer of the two, Ti2–OT2, clearly reduces in length while the shorter one, Ti1–OT2, appears to increase slightly, as shown in figure 5. (In the case of Ti1–OT2 there is a significant offset between the values obtained at ambient pressure and 0.2 GPa. The trend in this bond length is taken relative to the 0.2 GPa reference point.) These changes reduce the difference between the Ti1–OT2 and the Ti2–OT2 bond lengths by around 20%, but the Ti1–OT1 and Ti2–OT1 bonds appear to retain their bond length difference; it would now be of interest to find out whether there is any accompanying variation in the second-harmonic generating (SHG) properties as a function of pressure. From table 2, it is also evident that the relatively long Ti1–O5 and Ti2–O3 bonds undergo significant shortening under pressure (relative to the 0.2 GPa values). As indicated above, however, the shortening of these bonds does not significantly reduce the overall distortions of the TiO_6 octahedra.

The orientation of the Ti–O bonds, as well as the variation of their bond lengths, is also considered to be important for the non-linear optical properties of the KTP structure [1, 24, 25]. In the calculation of the non-linear tensor coefficients, the

Table 4. Selected P–O–Ti and Ti–OT–Ti bond angles (°) in $KTiOPO_4$ as a function of pressure. The atmospheric-pressure (AP) values were calculated from the refined atomic fractional coordinates of Thomas *et al* [1].

	Pressure (GPa)				
	AP [1]	0.2 GPa	2.2 GPa	3.7 GPa	4.7 GPa
P1–O3–Ti2	129.6(2)	131.0(7)	129.8(7)	128.2(7)	128.1(5)
P2–O7–Ti2	130.3(2)	132.9(9)	130.3(9)	126.6(9)	128.9(9)
P1–O4–Ti2	134.8(2)	132.9(7)	132.3(7)	131.9(7)	132.4(6)
P2–O6–Ti1	135.9(2)	136.6(9)	136.1(9)	134.8(9)	134.8(9)
Ti1–OT2–Ti2	133.4(2)	134.6(9)	133.6(8)	134.3(8)	133.5(7)

orientations of the bonds participate through products of their direction cosines, where the direction cosines are determined with respect to the crystallographic axes [25]. For the KTP structure the distortions of the TiO_6 octahedra give rise to an inherently asymmetric summation of the direction cosines along the polar axis of the crystal. Although the TiO_6 octahedra appear to be tilting with respect to the PO_4 tetrahedra, the magnitude of this re-orientation does not affect the summation of the direction cosines significantly.

As already outlined, the KTP structure assumes a pronounced pseudosymmetry derived from the centric $Pnan$ space group [1], and it is of interest to examine how the structure moves with respect to this space group as the phase transition at 5.5 GPa is approached. In order to do so the Missym computer program [1, 26] was utilized to compare the refined coordinates with the pseudosymmetry at all four pressures. The degree of pseudosymmetry was found to remain almost constant and, therefore, the structure neither appeared to be moving significantly towards or away from the prototypic $Pnan$ phase. It is also interesting to note that the Missym program did not indicate an approach towards any other pseudosymmetries at 4.7 GPa, suggesting that the structural transition is first-order in character.

The deformation of the TiO_6–PO_4 framework is not accompanied by a significant movement of the titanium atoms (table 1) although, as already indicated, there is a clear movement of the phosphorus atoms and a change in the P–O–Ti bond angles. Since the O–Ti–O angles show changes of 2° or less (to 4.7 GPa) the titanium octahedra remain fairly rigid in shape. Therefore the movement of the phosphorus atoms relative to the stationary titanium atoms, coupled with the angular changes in the P–O–Ti linking bond angles, suggest that the TiO_6 octahedra are tilting relative to the PO_4 tetrahedra.

The observed structural changes of KTP as it approaches its phase transition are similar in kind to those of the plagioclase feldspar anorthite $CaAl_2Si_2O_8$ which exhibits a first-order structural phase transition at 2.6 Gpa [23]. All of the feldspars have crystal structures consisting of a three-dimensional framework of corner-linked AlO_4 and SiO_4 tetrahedra. In the case of anorthite, cavities formed in the framework, which are analogous to the cage sites of KTP, contain Ca atoms. The mechanism for the transition, from the low-pressure $P\bar{1}$ structure to the $I\bar{1}$ high-pressure structure, is tilting of the essentially rigid tetrahedra of the framework. The resulting deformation of the framework from the ambient structure apparently reflects a need to accommodate both the applied pressure and the large Ca cations within the cavities of the framework. Initially the volumes of the cavities, as defined by the eight closest

oxygen positions, decrease under pressure in a manner similar to that of the cage sites in KTP. After the transition the volume of the cavities increases again as the framework tetrahedra suddenly tilt into new orientations. The tilting of the tetrahedra manifests itself as a change of the T–O–T (Al, Si–O–Al, Si) bond angles, which link neighbouring tetrahedra. The magnitudes of the T–O–T bond angle changes between atmospheric pressure and the phase transition are of the same order as those for the P–O–Ti linking bonds of KTP. After the transition in anorthite, however, there is a sudden angular change of the linking bonds with one such bond exhibiting an increase of 17°, where it had initially decreased by only 2° as the phase transition was approached. It is also interesting to note that the Ca atom environments, or rather the potential well within each cavity, show a marked change above the phase transition. In the low-pressure phase the potential within the cavities is wide and relatively flat while above the transition the potential becomes significantly sharper. Although the KTP cage sites are quite different from the anorthite cavities, the high-pressure Raman study and the present high-pressure structural study both indicate that a significant pressure dependence is present for the K atom environments as the phase transition is approached. The Raman study provides additional evidence that the potential well within the cage sites also becomes sharper after the transition, in as much as the initially softening 56 cm^{-1} mode becomes stiffer. However, it remains to be seen whether the cage sites increase their volume after the transition in a manner similar to that of anorthite.

The observed decrease of the K-cage site volumes under pressure intuitively suggests that the potential experienced by the K atoms will sharpen under pressure, thereby coupling the motion of the K atoms more closely to that of the cage oxygens. But in the absence of a detailed analysis of the phonon spectrum it is not possible to relate the observed structural changes of KTP with pressure to the softening 56 cm^{-1} A_1 mode. However, the tilting of the TiO_6 octahedra relative to the PO_4 tetrahedra does generally agree with the behaviour proposed by Kourouklis *et al* [9] as the phase transition is approached.

4. Conclusions

The principal changes of the KTP structure under pressure are in the region of the relatively compressible K cages. The PO_4 and TiO_6 units remain rigid in size and shape, and the compression of the cages appears to be accommodated by significant buckling of the framework structure, accompanied by a pronounced movement of the K2 atom. The observed angular changes in the P–O–Ti linking bonds suggest that the deformation of the structure around the the cage sites is principally achieved by tilting of the TiO_6 octahedra relative to the PO_4 tetrahedra.

The other structural changes up to 4.7 GPa are relatively small. In particular, the TiO_6 octahedra were found to retain their general distortion although there are some small changes in Ti–O distances, including a reduction in the difference between the Ti1–OT2 and Ti2–OT2 bond lengths. It is not known whether the SHG properties—thought to be associated with the distorted TiO_6 octahedra—remain unaltered with pressure and a study is being planned to determine this. The results of the analysis with the Missym program indicate that the changes in the structure are consistent with a first-order phase transition and it is not possible to predict the structure of the high-pressure phase. Therefore it is proposed to continue the study of the KTP structure through the phase transition.

Acknowledgments

We are grateful to Mr H Vass and Mr S Duffield for their technical assistance and to Dr P D Hatton, Dr R O Piltz and Dr R J Angel for many useful discussions. In particular, we thank Dr Angel for drawing our attention to the probable similarities between KTP and anorthite. This work is supported by a grant from the UK Science and Engineering Research Council.

References

[1] Thomas P A, Glazer A M and Watts B E 1990 *Acta Crystallogr.* B **46** 333–43
[2] Tordjman I, Masse R and Guitel J C 1974 *Z. Kristallogr., Bd.* **139** 103–15
[3] Masse R and Grenier J 1971 *Bull. Soc. Fr. Mineral. Crystallogr.* **94** 437–42
[4] El Brahimi M and Durand J 1986 *Rev. Chim. Miner.* **23** 146–53
[5] Slobodyanik N S, Nagornyi P G, Skopenko V V and Lugovskaya E S 1987 *Russ. J. Inorg. Chem.* **32** 1023–6
[6] Phillips M L, Gier T E, Eddy M M, Kedder N L, Stucky G D and Bierlien J D 1989 *Solid State Ionics* **32/33** 147–53
[7] Stucky G D, Phillips M L F and Gier T E 1989 *Chem. Mater.* **1** 492–509
[8] Harrison W T A, Gier T E, Stucky G D and Schultz A J 1990 *J. Chem. Soc., Chem. Commun.* **7** 540–2
[9] Kourouklis G A, Jayaraman A and Balliman A A 1987 *Solid State Commun.* **62** 379–82
[10] Pisarev R V, Farhi R, Moch P and Voronkova V I 1990 *J. Phys.: Condens. Matter* **2** 7555–68
[11] Nelmes R J, Loveday J S, Kaldis E and Karpinski J 1990 *Physica* C **172** 311–24
[12] Finger L W and King H E 1978 *Am. Min.* **63** 337
[13] Loveday J S, McMahon M I and Nelmes R J 1990 *J. Appl. Crystallogr.* **23** 392
[14] King H E and Finger L W 1981 *High Pressure Crystallography with a CAD4* Instruction manual (Delft: Enraf-Nonius)
[15] Zucker U H, Perenthaler E, Kuhs W F, Buchmann R and Schulz H 1983 *J. Appl. Crystallogr.* **16** 358
[16] Prince E and Nicholson W L 1985 *Structure and Statistics in Crystallography* ed A J C Wilson (New York: Adenine) pp 183–6
[17] Hazen R M and Finger L W 1989 *Am. Min.* **74** 352
[18] Lehmann M S 1975 *J. Appl. Crystallogr.* **8** 165
[19] *International Tables For X-ray Crystallography* vol 4 pp 288–92
[20] Hamilton W C 1964 *Statistics in Physical Science* (New York: Ronald)
[21] King H E and Finger L W 1979 *J. Appl. Crystallogr.* **12** 374
[22] Ida Y 1985 *Volfit* (program) Institute for Solid State Physics, University of Tokyo
[23] Angel R J 1988 *Am. Min.* **73** 1114–9
[24] Hansen N K, Protas J and Marnier G 1988 *C. R. Acad. Sci.* **307**(II) 475–9
[25] Sastry P U M 1991 *Solid State Commun.* **78** 593–7
[26] Le Page Y 1988 *J. Appl. Crystallogr.* **21** 983–4